ELSEVIER

MCN Molecular and Cellular Neuroscience

www.elsevier.com/locate/ymcne
Mol. Cell. Neurosci. 35 (2007) 501–512

Marlin-1 and conventional kinesin link $GABA_B$ receptors to the cytoskeleton and regulate receptor transport

René L. Vidal,[a,d] Omar A. Ramírez,[a] Lisette Sandoval,[a,d] Roger Koenig-Robert,[a] Steffen Härtel,[b] and Andrés Couve[a,c,*]

[a]*Physiology and Biophysics, ICBM, Faculty of Medicine, Universidad de Chile Independencia 1027, Santiago, Chile*
[b]*Anatomy and Development, ICBM, Faculty of Medicine, Universidad de Chile Independencia 1027, Santiago, Chile*
[c]*Center for Integrated Neurosciences (CENI) Universidad de Chile Independencia 1027, Santiago, Chile*
[d]*Institute of Biochemistry, Universidad Austral de Chile, Isla Teja, Valdivia, Chile*

Received 14 December 2006; revised 10 April 2007; accepted 25 April 2007
Available online 1 May 2007

The cytoskeleton and cytoskeletal motors play a fundamental role in neurotransmitter receptor trafficking, but proteins that link $GABA_B$ receptors ($GABA_BRs$) to the cytoskeleton have not been described. We recently identified Marlin-1, a protein that interacts with $GABA_BR1$. Here, we explore the association of $GABA_BRs$ and Marlin-1 to the cytoskeleton using a combination of biochemistry, microscopy and live cell imaging. Our results indicate that Marlin-1 is associated to microtubules and the molecular motor kinesin-I. We demonstrate that a fraction of Marlin-1 is mobile in dendrites of cultured hippocampal neurons and that mobility is microtubule-dependent. We also show that $GABA_BRs$ interact robustly with kinesin-I and that intracellular membranes containing $GABA_BRs$ are sensitive to treatments that disrupt a protein complex containing Marlin-1, kinesin-I and tubulin. Finally, we report that a kinesin-I mutant severely impairs receptor transport. We conclude that Marlin-1 and kinesin-1 link $GABA_BRs$ to the tubulin cytoskeleton in neurons.

Keywords: $GABA_B$; Marlin-1; Microtubules; Neurons; Cytoskeleton; FRAP

Introduction

Neurotransmitter receptors are directly responsible for synaptic transmission and constitute key elements in the modulation of synaptic plasticity. In neurons, neurotransmitter receptors are precisely located at synaptic or extrasynaptic sites in pre or post-synaptic terminals (Craig and Boudin, 2001). In this context, the regulation of trafficking, which includes transport, assembly, insertion, anchoring, recycling and degradation of neurotransmitter receptors results in the modification of receptor number at these sites (Bailey et al., 2004; Collingridge et al., 2004). For example, it has been firmly established both *in vitro* and *in vivo* that synaptic activity and experience modify the trafficking of ionotropic glutamate receptors (Clem and Barth, 2006; Collingridge et al., 2004). Likewise, evidence from cultured systems has indicated that trafficking of ionotropic $GABA_A$ receptors alters the strength of inhibitory synapses (Kittler et al., 2002). In most cases accessory proteins participate in the trafficking of neurotransmitter receptors and frequently act as intermediaries or adaptors between receptors and the underlying cytoskeleton. Adaptor proteins have been described for ionotropic and metabotropic glutamate receptors, and for $GABA_A$ receptors (Collingridge et al., 2004; Moss and Smart, 2001). On the contrary, proteins that mediate the association of $GABA_B$ receptors ($GABA_BRs$) to the cytoskeleton remain for the most part unidentified.

$GABA_BRs$ are G protein-coupled receptors (GPCRs) that control the slow component of inhibitory neurotransmission. Multiple reports have now demonstrated that a single functional heterodimer composed of $GABA_BR1$ and $GABA_BR2$ mediates the coupling to adenylyl cyclase, voltage-gated Ca^{2+} channels and inwardly rectifying K^+ channels, the known effectors of $GABA_BRs$ (Bettler et al., 2004; Mott and Lewis, 1994). The $GABA_BR$ heterodimer displays unique functional properties, somewhat anomalous for the canonical GPCR paradigm. These may be summarized as follows: $GABA_BR1$ contains a RXR type sequence (RSRR) located in its carboxyl terminal domain that functions as an endoplasmic reticulum (ER) retention motif. The motif is masked upon assembly with $GABA_BR2$, and the assembled heterodimer exits the ER and it is exocytosed onto the cell surface (Couve et al., 2004b). The two subunits are not functionally equivalent as only $GABA_BR1$ binds GABA with high affinity whereas $GABA_BR2$ mediates coupling to G proteins (Pin et al.,

Abbreviations: CNS, central nervous system; Ccs, coiled-coil domains; ER, endoplasmic reticulum; bp, base pair.

* Corresponding author. Programa de Fisiología y Biofísica, ICBM, Facultad de Medicina, Universidad de Chile, Independencia 1027, Santiago, Chile. Fax: +56 2 777 6916.
E-mail address: andres@neuro.med.uchile.cl (A. Couve).
Available online on ScienceDirect (www.sciencedirect.com).

1044-7431/$ - see front matter © 2007 Elsevier Inc. All rights reserved.
doi:10.1016/j.mcn.2007.04.008

2004). This sophisticated modulation of $GABA_BRs$ suggests that receptor abundance and distribution are tightly controlled in neurons. Several proteins that associate to $GABA_BRs$ have been described (Couve et al., 2004b). Among them 14-3-3, msec-7 and NSF have been suggested to control receptor trafficking (Couve et al., 2001; Restituito et al., 2005; Brock et al., 2005; Pontier et al., 2006). However, they are general secretory pathway factors and their precise relationship to the cytoskeleton has not been reported (Tan et al., 2004).

In order to contribute to the characterization of proteins that modulate aspects of the biosynthetic pathways of $GABA_BRs$ we recently carried out a yeast two-hybrid screen using the intracellular domain the $GABA_BR1$ subunit and reported the identification of Marlin-1 (Couve et al., 2004a). Marlin-1 belongs to a new family of three related proteins, which are highly conserved in vertebrates. It contains putative nuclear localization and nuclear export signals, but it is predominantly cytoplasmic in neurons of the central nervous system (CNS). Marlin-1 contains multiple coiled-coil domains (Ccs) arranged along the entire length of the protein with two leucine-zippers in the carboxyl terminal region of the molecule. It is interesting to note that the Ccs of Marlin-1 provide binding specificity to different molecular partners. Ccs usually mediate protein interactions (Burkhard et al., 2001) and the modular set of interactions displayed by Marlin-1 is reminiscent of adaptor proteins. The tissue distribution of Marlin-1 is not ubiquitous. Northern and western blot analyses have shown that Marlin-1 is expressed primarily in the brain. In cortical and hippocampal neurons depletion of Marlin-1 results in the accumulation of the $GABA_BR2$ subunit. These observations demonstrate that Marlin-1 affects the abundance of $GABA_BRs$ but do not shed light on the exact mechanism of action. Studies in non neuronal cell lines have indicated that Marlin-1 associates with the group of Janus kinases and microtubules (Steindler et al., 2004). However, the interaction between Marlin-1 and the cytoskeleton has not been explored in neurons and the role of Marlin-1 in $GABA_B$ receptor trafficking has not been addressed.

Here we hypothesize that Marlin-1 associates to microtubules in the brain and modulates the trafficking of $GABA_BRs$ by interacting with the cytoskeleton. We provide evidence that native Marlin-1 associates with microtubules in the brain. Furthermore, we show that Marlin-1 is a mobile protein in neurons and that intracellular movement depends on microtubule integrity. In addition, we demonstrate that Marlin-1 and $GABA_BR1$ interact with conventional kinesin (kinesin-I), a plus end microtubule-dependent molecular motor, thus providing a molecular mechanism for mobility in neurites. We show that Marlin-1, like tubulin and kinesin-I, associates to intracellular membranes in the brain and that removal of the complex alters an intracellular compartment containing $GABA_BRs$. Finally, we demonstrate that kinesin-I modulates the transport of $GABA_BR1$. Thus, we suggest that Marlin-1 and kinesin-I participate in the association of $GABA_B$ receptors to the dynamic cytoskeleton.

Results

Marlin-1 associates with microtubules in the brain

Marlin-1 is present in the soma and neurites of hippocampal neurons (Couve et al., 2004a). Occasionally, the presence of a fibrous staining pattern has been observed in neurons, but the distribution relative to the cytoskeleton has not been reported. To determine whether Marlin-1 is associated to the cytoskeleton in the brain we began exploring the association to microtubules. We used an antibody to Marlin-1 that has been characterized previously and that recognizes specifically the C-terminal domain of the protein (Couve et al., 2004a and Supplementary Figs. 1A and B).

A microsomal fraction enriched in Marlin-1 was prepared and the sensitivity to cytoskeletal disrupting agents was evaluated by monitoring the abundance of Marlin-1 in the soluble and insoluble fractions before and after treatment. Under control conditions Marlin-1 distributed mainly to the pellet (insoluble fraction) and was absent from the soluble pool (M1, Fig. 1A, top, lanes 1 and 2). Upon treatment with Taxol, a drug known to stabilize polymerized microtubules, Marlin-1 remained in the pellet (M1, Fig. 1A, top, lanes 3 and 4). On the contrary, treatment with nocodazole, an agent that destabilizes microtubules, resulted in the complete shift of Marlin-1 to the soluble fraction (M1, Fig. 1A, top, lanes 5 and 6). To correlate the behavior of Marlin-1 to the state of tubulin polymerization the samples were also immunoblotted for β-tubulin. Under control conditions β-tubulin distributed between the pellet and the soluble fraction (Fig. 1A, bottom, lanes 1 and 2). Upon treatment with Taxol β-tubulin shifted completely to the pellet (Fig. 1A, bottom, lanes 3 and 4). Conversely, treatment of the sample with nocodazole, resulted in the enrichment of β-tubulin in the soluble fraction (Fig. 1A, bottom, lanes 5 and 6).

To confirm the association between Marlin-1 and microtubules a fraction containing soluble Marlin-1 and depolymerized β-tubulin was subject to a second cycle of polymerization. As shown above, β-tubulin and Marlin-1 were released from the pellet in the first cycle of nocodazole treatment (Fig. 1B, lanes 3 and 4). More importantly, when the solubilized fraction was treated with Taxol, β-tubulin and Marlin-1 were re-precipitated and appeared exclusively in the pellet (Fig. 1B, lanes 5 and 6). Taken together, these observations demonstrate that endogenous Marlin-1 associates with polymerized microtubules in rat brains preparations.

Marlin-1 co-localizes with microtubules in hippocampal neurons

To directly visualize the interaction between Marlin-1 and β-tubulin the distribution of both proteins was compared by immunofluorescence in cultured hippocampal neurons. Stage 2–3 hippocampal neurons (0.5–1.5 div; Goslin and Banker, 1991) were used to facilitate the distinction of discrete tubulin fibers or tracks in nascent neurites. The distribution of tubulin concentrated in the periphery of the soma and in tracks within the shaft neurites (Figs. 1C and D). The staining of Marlin-1 was consistent with previous reports and showed prominent punctate staining in the soma and proximal neurites (Couve et al., 2004a). More importantly, Marlin-1 puncta decorated tubulin tracks in developing projections (Figs. 1C and D). To demonstrate the specificity of the decoration a control staining was carried out with actin. As expected actin did not form puncta in association with Marlin-1 or β-tubulin fibers and instead was enriched in the growth cone of the processes (Figs. 1E and F). These observations show that Marlin-1 co-localizes with tubulin fibers in hippocampal neurons and complement the biochemical association described above.

Marlin-1 is highly mobile in hippocampal neurons

The association to microtubules suggests that Marlin-1 may display cytoskeleton-dependent mobility in polarized cells. To begin addressing this issue we generated an EGFP-tagged version of Marlin-1 (Marlin-1–EGFP) and performed fluorescence recovery after photobleaching (FRAP) in live neurons. First, to validate

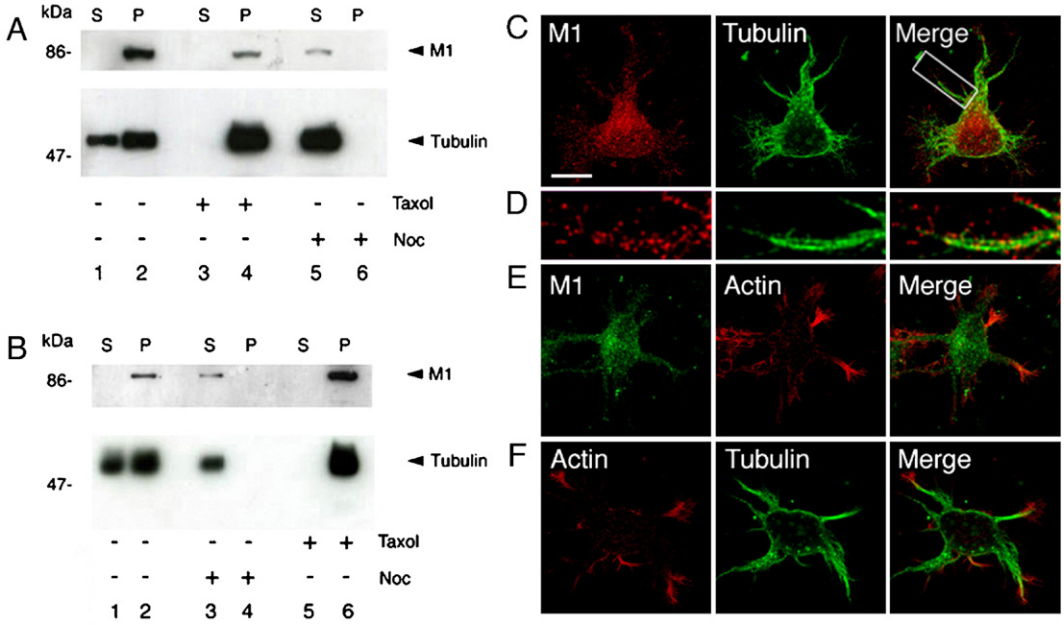

Fig. 1. Marlin-1 associates with microtubules. (A) Rat brains were homogenized and a high-speed fraction enriched in Marlin-1 was prepared (P). A soluble pool was also collected (S). Samples were left untreated (lanes 1 and 2), treated with 20 μM Taxol for 40 min at RT (lanes 3 and 4), or treated with 10 μM nocodazole (Noc) for 40 min at RT (lanes 5 and 6). Samples were separated by SDS–PAGE and transferred to a nitrocellulose membrane. The membrane was used for immunoblots with purified anti-Marlin-1 (M1, top) or anti-β-tubulin (bottom) primary antibodies and HRP conjugated secondary antibodies. Positions of molecular weight standards are indicated on the left-hand side. (B) The procedure was repeated with an extra cycle of depolymerization/polymerization. Briefly, rat brains were homogenized and a high-speed fraction was prepared (P). A soluble pool was also collected (S). Samples were left untreated (lanes 1 and 2) or treated with 10 μM nocodazole (Noc) for 40 min at RT (lanes 3 and 4). After nocodazole treatment the soluble fraction from lane 3 was treated with 20 μM Taxol for 40 min at RT to re-precipitate microtubules (lanes 5 and 6). Positions of molecular weight standards are indicated on the left-hand side. Immunoblots were performed as described above. (C) Stage 2–3 hippocampal neurons were fixed and stained with anti-Marlin-1 (M1) and anti-β-tubulin antibodies followed by Texas Red and FITC secondary antibodies. The merge panel is shown on the right. (D) Higher magnification of the region boxed in panel C. (E) Same as above with neurons fixed and stained with anti-Marlin-1 and anti-actin. (F) Same as above with neurons fixed and stained with anti-actin and anti-β-tubulin antibodies. All images were obtained using a Zeiss confocal microscope and processed by deconvolution. Scale bars, (C) 10 μm.

our approach Marlin-1–EGFP was transfected into hippocampal neurons and cells were imaged by confocal microscopy to compare the subcellular distribution of native and recombinant proteins. Importantly, the distribution of Marlin-1–EGFP resembled the endogenous protein (Figs. 2A and B). Marlin-1–EGFP was excluded from the nucleus and was abundant in the cell body and proximal dendrites, where a fine punctate staining was observed. As reported earlier for the endogenous protein and for FLAG–Marlin-1 (Couve et al., 2004a), larger accumulations were occasionally visible in the soma and dendrites of transfected neurons. Their distribution was also compared by co-staining with anti-Marlin and anti-GFP antibodies. The pattern shows significant overlap indicating that the recombinant protein mimics the distribution of endogenous Marlin-1 (Figs. 2C1–C3). As expected, the subcellular distribution of EGFP differed significantly and filled the nucleus and cytoplasm of transfected neurons (Fig. 2B, inset).

Next, taking advantage of its distribution in neuronal dendrites, Marlin-1–EGFP was used to study protein mobility via FRAP. Only neurons with a fine punctate staining were selected for the assay. After photobleaching a region of interest (ROI) from a chosen dendrite, the relative fluorescence of Marlin-1–EGFP diminished and subsequently recovered significantly (Figs. 2D–F, arrowhead and 2G). A non-photobleached dendrite and the background remained stable for the duration of the experiment indicating that recovery is specific for the photobleached area (Fig. 2G). These results demonstrate that a significant proportion of Marlin-1–EGFP is mobile in dendrites of hippocampal neurons in culture. To determine the direction of movement we measured the kinetics and extent of recovery on both extremes of the photobleached area. To allow a direct comparison of recovery the normalized fluorescence was used for this and subsequent analyses. The results clearly indicate that recovery is identical on both extremes suggesting that the mobility of Marlin-1–EGFP is bidirectional (Fig. 2H).

To evaluate the properties of mobility the recovery of Marlin-1–EGFP and EGFP were compared. Importantly, Marlin-1–EGFP recovered significantly slower than EGFP ($t_{1/2}$ Marlin-1–EGFP≈150 s, $t_{1/2}$ EGFP≈15 s, Fig. 3). In addition, Marlin-1–EGFP recovered only ~47% whereas EGFP reached ~95% of the original fluorescence. These observations suggest that mobile and immobile populations of Marlin-1–EGFP exist in neurons. In addition, they show that the mobile pool of Marlin-1–EGFP is restricted in dendrites when compared to EGFP.

The mobility of Marlin-1 is microtubule-dependent

To determine whether microtubules play a role in Marlin-1–EGFP mobility, the experiment was performed in the presence of nocodazole. In agreement with the microtubule association assays described above, disrupting the tubulin cytoskeleton significantly affected the mobility of Marlin-1–EGFP in neurons. Thus, in the

presence of nocodazole there was no detectable recovery of Marlin-1–EGFP fluorescence (Figs. 3A–C). On the contrary, nocodazole had no effect of the mobility of soluble EGFP (Fig. 3C). These experiments conclusively demonstrate that the mobile pool of Marlin-1–EGFP depends on an intact microtubule cytoskeleton.

Marlin-1 and $GABA_BRs$ interact with conventional kinesin

The microtubule network is highly organized in neurons. Microtubules orient their plus ends towards the neurite tip in axons and distal dendrites, whereas they show a mixed polarity in proximal dendrites (Hirokawa and Takemura, 2005). The microtubule-based movement in neurons is controlled by two large groups of molecular motors, i.e. dyneins and kinesins. This organization allows the directional transport of molecules along neuronal projections. If the bidirectional movement of Marlin-1–EGFP is mediated by molecular motors, two possibilities exist. Either Marlin-1–EGFP is transported bidirectionally by one class of molecular motor in proximal dendrites (mixed polarity) or our experiments include plus and minus end motors travelling in opposite directions. To provide information regarding the participation of molecular motors and define the particular type involved we evaluated their association to

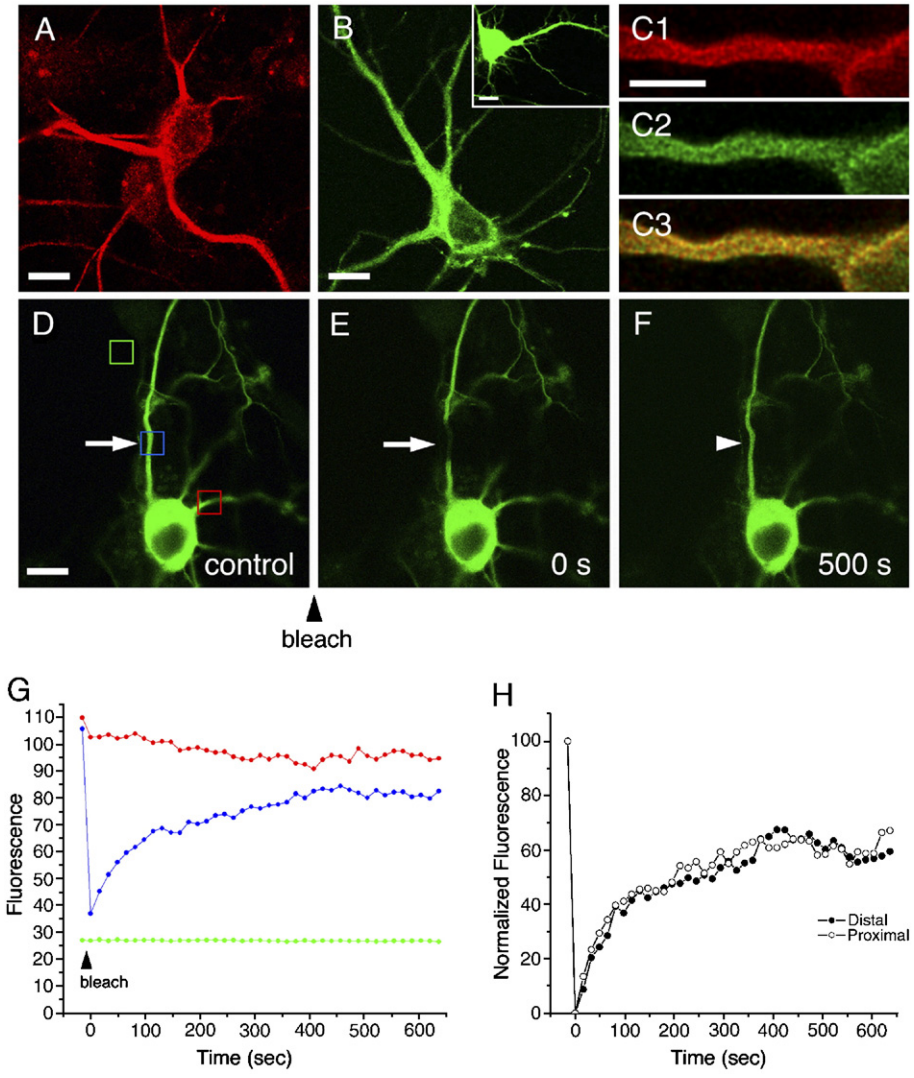

Fig. 2. Marlin-1 is highly mobile in hippocampal neurons. (A) 8–10 div hippocampal neurons were stained for endogenous Marlin-1 with rabbit anti-Marlin-1 antibodies and secondary anti rabbit Texas Red antibodies. (B) 8–10 div hippocampal neurons were transfected with Marlin-1-EGFP or EGFP (inset) and imaged by confocal microscopy 48 h after transfection. Scale bars (A and B), 10 μm. (C) 8–10 div hippocampal neurons were transfected with Marlin-1–EGFP and stained with anti-Marlin-1 (C1) and anti-GFP (C2). (C3) Merge panel. Scale bar (C1), 5 μm. (D–F) FRAP analysis in a 8–10 div hippocampal neuron expressing Marlin-1–EGFP. (D) Regions of interest (ROIs) were placed over an experimental dendrite (blue), a control dendrite (red) and the background area (green). (E) The experimental ROI in blue was photobleached. The result of photobleaching can be seen within microns of the soma (arrow). (F) 40 consecutive frames were acquired using a confocal microscope over a period of approximately 10 min. A selected frame in the time series after ~500 s is shown. The final recovery of the dendritic region is shown (arrowhead). Scale bars (D), 10 μm. (G) Raw fluorescent intensity (arbitrary units) corresponding to the regions shown in colored boxes in panel D. Green, background; blue, bleached dendrite; red non-bleached dendrite from the same neuron. (H) The normalized mean intensities of the recovered regions at a distance of 0.5 μm of either edge of the photobleached area were obtained for each time frame. The average of fluorescence recovery for each frame was plotted against time. Filled circles, distal side relative to the soma; empty circles, proximal side of the same neurite.

Marlin-1 by immunoprecipitation. Interestingly, Marlin-1 immunoprecipitated with conventional kinesin-I but not with kinesin-II or dynein (Fig. 4A, top three panels). The specificity of kinesin-1 detection was further confirmed by immunoblots in the absence of primary antibody where only the light chains of the IgG from the immunoprecipitation were observed (Fig. 4A, bottom panel). Co-immunoprecipitation assays from transiently transfected COS-7 cells also indicated that kinesin-I interacted with the N-terminal domain of Marlin-1 (Cc1), but not with the middle (Cc2) or C-terminal domains (Cc3) responsible for binding RNA, $GABA_BRs$ and Janus kinases (Fig. 4B). Taken together these experiments demonstrate that Marlin-1 is associated with kinesin-I and suggest that the movement of Marlin-1 is mediated by plus end microtubule-dependent molecular motors.

These results raised the possibility that molecular motors, in particular kinesin-I, mediate the transport of $GABA_B$ receptors in neurons. To start addressing this issue the interaction between kinesin-I and $GABA_B$ receptors was evaluated by immunoprecipitation from rat brain extracts. Importantly, $GABA_BR1$ co-immunoprecipitated with kinesin-I (Fig. 4C, top panel, lanes 3–5) but not with a different molecular motor, namely dynein (Fig. 4C, bottom panel, lanes 3–5). The immunoprecipitation was reproduced with different $GABA_BR1$ antibodies, was resistant to high salt concentration (500 mM NaCl) and occurred in RIPA buffer (data not shown). In addition, the specificity of kinesin-I detection was confirmed by immunoblots in the absence of primary antibody where no kinesin-I bands are visible (Fig. 4C, lanes 1 and 2).

In general, the association of neurotransmitter receptors and kinesin type motors occurs primarily in dendritic shafts (Hirokawa and Takemura, 2005). Thus, to gain insight into the subcellular localization of $GABA_BR1$ and kinesin-I complexes, we evaluated the distribution of both proteins by confocal microscopy in cultured hippocampal neurons. As reported previously, kinesin-I distributed in the soma and projections of cultured neurons (data not shown) and accumulated in dense structures that did not resemble the microtubular network (Pfister et al., 1989). Interestingly, high-magnification images show that a proportion of $GABA_BR1$ and kinesin-1 co-localize predominantly in peripheral structures within dendrites of hippocampal neurons (Fig. 4D, top panels). This spatial association is specific as demonstrated by the lack of co-localization with dynein (Fig. 4D, bottom panels).

Finally, an experiment in a heterologous expression system demonstrated that $GABA_BR1$ co-immunoprecipitated with Marlin-1 and kinesin-I, providing evidence for the existence of a complex between these proteins (Fig. 4E).

The intracellular pool of $GABA_BRs$ is sensitive to alterations of the cytoskeleton

The interaction between $GABA_BR1$, Marlin-1, microtubules and kinesin-I suggests that a motor complex may participate in the intracellular movement of $GABA_BRs$ in neurons. In this context, it is conceivable that the motor complex will regulate $GABA_BR$ trafficking or subcellular localization. To begin exploring these possibilities a subcellular fractionation study of adult brain homogenates was carried out to determine the subcellular distributions of these proteins. Importantly, Marlin-1 was abundant in a soluble post mitochondrial fraction (S2) and precipitated in a high-speed microsomal pellet containing light intracellular membranes (P3) (Lee et al., 2001) (Fig. 5E, lanes 1–4). The absence of Marlin-1 in S3 (Fig. 5E, lane 3) indicates that the protein does not exists in free form, but that is primarily associated to membranes or large macromolecular complexes. On the contrary kinesin-I is abundant in S3 and P3 (Fig. 5E, lanes 3–4). $GABA_BRs$ were more abundant in a crude membrane fraction (P2) but were also present in the post mitochondrial fraction (S2) that precipitated as a microsomal pellet (P3) (Fig. 5E, lanes 1–4). These observations are in agreement with the abundant intracellular distribution of $GABA_BR1$ and $GABA_BR2$

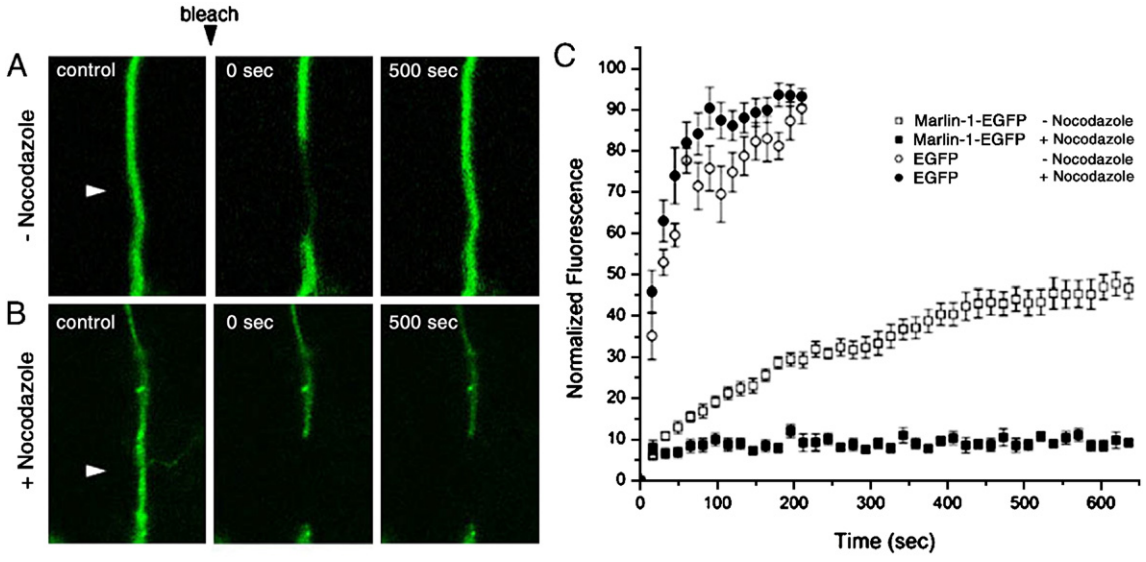

Fig. 3. The mobility of Marlin-1 depends on microtubules. (A) Example of FRAP of Marlin-1–EGFP in a selected dendrite under control conditions. After photobleaching an area of interest (white arrowhead), 40 consecutive frames were acquired using a confocal microscope over a period of approximately 10 min. Selected frames in the time series before bleaching (control), at times 0 and 500 s after bleaching are shown. (B) Example of FRAP of Marlin-1–EGFP in a selected dendrite after nocodazole treatment. (C) FRAP analysis in hippocampal neurons transfected with EGFP or Marlin-1–EGFP. The normalized mean intensity of a photobleached/recovered region was obtained for each time frame. The average fluorescence recovery was plotted against time. EGFP (empty circles), Marlin-1–EGFP (empty squares), EGFP + 100 μM nocodazole for 3 h (filled circles), Marlin-1–EGFP + 100 μM nocodazole for 3 h (filled squares). The data show the average of 8–10 independent measurements +/– S.E.M.

in neurons (Correa et al., 2004; Kulik et al., 2003). The Na^+/K^+ ATPase, a widely used marker for plasma membrane, was prominent in the crude membrane fraction (P2) (Fig. 5E, lane 2) and only a minor proportion was present in S2 and P3 (Fig. 5E, lanes 1 and 4). The predominance of the Na^+/K^+ ATPase in P2 and the absence of $GABA_BR1$ and the Na^+/K^+ ATPase in S3 demonstrate the effectiveness of the differential centrifugation procedure. These findings indicate that $GABA_BR1$, Marlin-1 and kinesin-I are present in a fraction enriched in light membranes consistent with the existence of an intracellular transport compartment (Lee et al., 2001).

To obtain a better resolution of these intracellular pools of proteins we explored their profiles by velocity sedimentation on

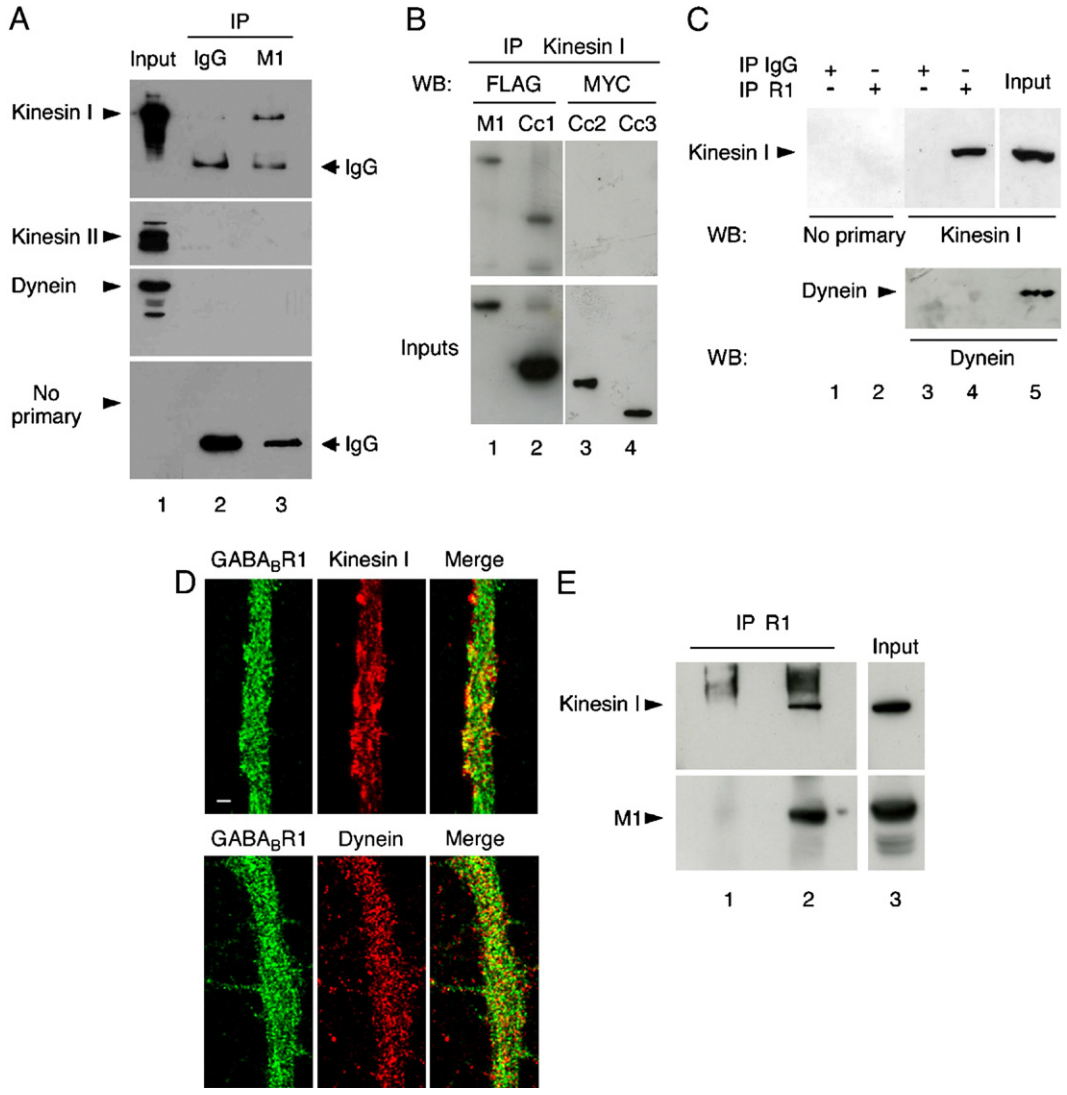

Fig. 4. Marlin-1 and $GABA_BR1$ interact with kinesin-I. (A) An S16 fraction was prepared from adult mouse brains. The S16 fraction prior to immunoprecipitations was used as loading control (input, lane 1). Samples were immunoprecipitated with control IgG (lane 2) or anti-Marlin-1 antibodies (M1, lane 3). Samples were separated by SDS–PAGE and immunoblotted with anti-kinesin-I, anti-kinesin-II, anti-dynein or no primary antibodies. Migration of IgGs used for immunoprecipitation is indicated on the right. (B) Co-immunoprecipitation of kinesin-I and domains of Marlin-1 in COS-7 cells. COS-7 cells were transfected with kinesin-I and FLAG–Marlin-1 (M1, lane 1) or the first Cc region of Marlin-1 also tagged with the FLAG epitope (Cc1, lane 2). Alternatively, COS-7 cells were transfected with kinesin-I and the second or third Cc regions of Marlin-1 tagged with the MYC epitope (Cc2 and Cc3, lanes 3 and 4, respectively). Samples were immunoprecipitated with anti-kinesin-I antibodies and immunoblotted with anti-FLAG or anti-MYC. Control lysates prior to immunoprecipitations were immunoblotted with anti-FLAG or anti-MYC antibodies (Inputs, bottom panels). (C) Brain extracts (S1) were immunoprecipitated with control IgG (lanes 1 and 3) or anti-$GABA_BR1$ antibodies (lanes 2 and 4). Control lysates prior to immunoprecipitations were used as loading controls (lane 5). Samples were separated by SDS–PAGE and immunoblotted with anti-kinesin-I (top panel, lanes 3–5), no primary (top panel, lanes 1 and 2) or anti-dynein antibodies (bottom panel, lanes 3–5). (D) Colocalization of $GABA_BR1$ and kinesin-I in cultured 18–21 div hippocampal neurons. Neurons were stained with anti-$GABA_BR1$ (left) and anti-kinesin-I (middle) antibodies (top panels) or with anti-$GABA_BR1$ and anti-dynein antibodies (bottom panels). FITC and Texas Red and conjugated secondary antibodies were used to visualize the proteins. Merge panels is shown on the right. Images were obtained using a Zeiss confocal microscope and processed by deconvolution. Scale bar, 2 μm. (E) Co-immunoprecipitation of $GABA_BR1$, kinesin-I and Marlin-1 in COS-7 cells. COS-7 cells were transfected with $GABA_BR1$-MYC (lane 1) or with $GABA_BR1$-MYC, kinesin-I and FLAG–Marlin-1 (lane 2). Samples were immunoprecipitated with anti-MYC antibodies and immunoblotted with anti-kinesin-I (top panel) or anti-FLAG to detect Marlin-1 (M1, bottom panel). Control lysates prior to immunoprecipitations were immunoblotted with anti-kinesin-I or anti-FLAG antibodies (lane 3).

discontinuous sucrose density gradients. Under control conditions Marlin-1 showed a broad distribution along the fractions of the gradient with a wide peak between fractions 5 and 8 (Figs. 5A and B). To investigate the properties of this peak, the P3 fraction was treated with various agents before loading the sucrose gradient. Interestingly, the profile changed dramatically upon treatment with the EDTA, a divalent cation chelator, and deoxycholate, an ionic detergent (Figs. 5A and B, and Supplementary Fig. 1C). On the contrary, the profile of Marlin-1 did not change significantly after treatment with nonionic detergents or RNAse (Supplementary Fig. 1C). These results confirm that Marlin-1 is not an integral membrane protein and indicate that is not tethered by RNA to components of P3 such as polysomes. Instead, they suggest that Marlin-1 sediments as part of a molecular complex, probably a protein complex, sensitive to Ca^{2+} or Mg^{2+}. The profiles of tubulin and kinesin-I show significant overlap with Marlin-1 on fractions 5–8 (Figs. 5A and C). Interestingly, both are also dissociated in the presence of EDTA. Tubulin, like Marlin-1, accumulates preferentially in fractions 1–3 of the gradient in the presence of EDTA (Fig. 5A). Kinesin-I on the contrary only shifts to lighter fractions (Figs. 5A and C). These results suggest that in a P3 fraction the molecular complexes containing Marlin-1, tubulin and kinesin-I show similar profiles and similar sensitivity to EDTA. Importantly, the intracellular pools of $GABA_BR1$ and $GABA_BR2$ also overlap with Marlin-1 and display EDTA sensitivity. Similar to kinesin-I, they only shift to fractions 2–7 instead of accumulating in the lightest fractions (Fig. 5A). These findings suggest that the intracellular membranes containing $GABA_BRs$ are stripped of unknown peripheral components in the presence of EDTA but retain kinesin-I. In view of the profile changes, our experiments suggest that Marlin-1, tubulin and kinesin-I are likely candidates to reside in the periphery of these intracellular membranes.

It has been demonstrated previously that Ca^{2+} and Mg^{2+} affect tubulin polymerization (Soto et al., 1996). To demonstrate that our EDTA treatment strips cytoskeletal components from $GABA_BR$ containing membranes, the P3 fraction was treated with nocodazole prior to loading the sucrose gradient. According to our hypothesis, after treatment with nocodazole tubulin and Marlin-1 shifted to fractions 1–3, consistent with the appearance of depolymerized microtubules (Fig. 5D and data not shown). More importantly, the intracellular membranes containing $GABA_B$ receptors displayed a shift in their profile similar to the one observed after EDTA treatment (Fig. 5D). These findings suggest that light membranes containing $GABA_BRs$ are bound to peripheral cytoskeletal elements which contain tubulin, kinesin-I and Marlin-1.

Kinesin-I modulates $GABA_B$ receptor transport

To study the relevance of the cytoskeleton and molecular motors in $GABA_BR$ trafficking, the subcellular distribution of $GABA_B$ receptors was analyzed in the presence of a mutant kinesin-I. Hippocampal neurons were co-transfected with the $GABA_BR1$ subunit and an EGFP vector encoding a version of kinesin-I lacking the stalk and cargo binding domains. By binding to microtubules, this truncated

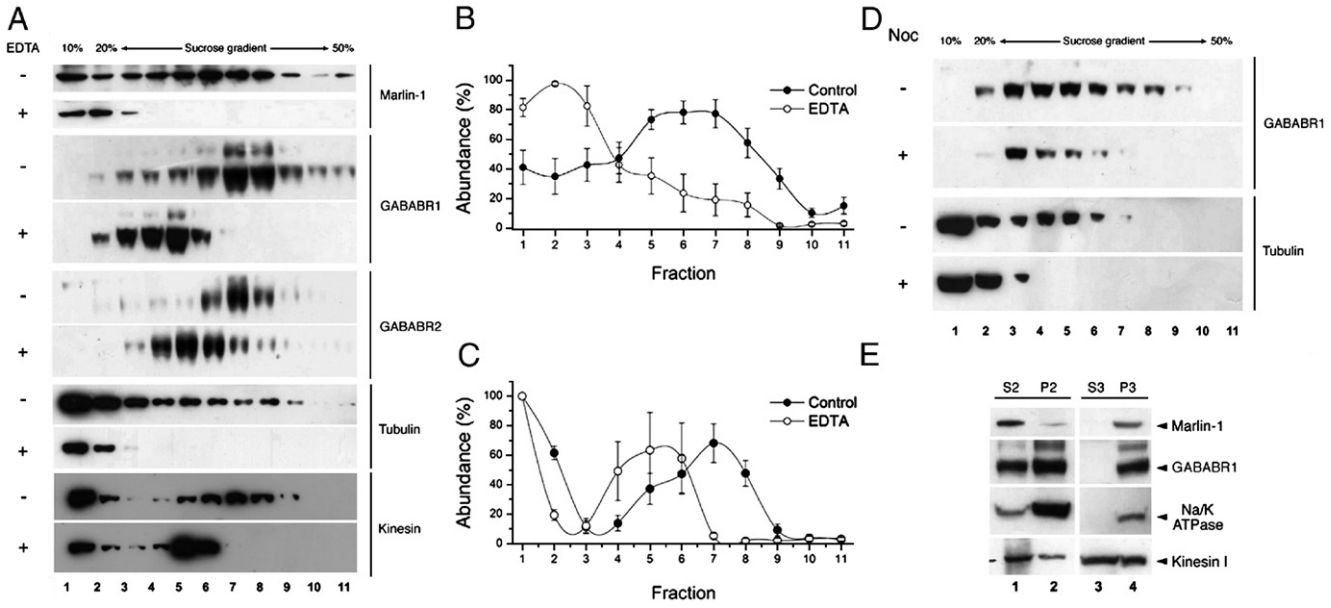

Fig. 5. $GABA_B$ receptors, Marlin-1, tubulin and kinesin display overlapping profiles after sucrose gradient analysis. (A) The P3 fraction derived from adult rat brains was separated by velocity sedimentation on a 10–50% discontinuous sucrose gradient under control conditions (−) or after 30 mM EDTA treatment (+). 11 fractions of equal volume were obtained and equal volumes were separated by SDS–PAGE and transferred to nitrocellulose (lanes 1–11). Nitrocellulose membranes were immunoblotted with anti-Marlin-1, anti-$GABA_BR1$, anti-$GABA_BR2$, anti-Na^+/K^+ ATPase, anti-tubulin or anti-kinesin-I antibodies. Fraction 1 is the lightest and fraction 11 is the heaviest of the gradient. (B) Immunoblots for Marlin-1 under control (filled circles) or EDTA treatment (open circles) were analyzed by densitometry and average values of normalized abundance±S.E.M. were plotted for each fraction ($n=7$ independent fractionation and sucrose gradient experiments). (C) Same as above for kinesin-I ($n=3$ independent fractionation and sucrose gradient experiments). (D) The P3 fraction derived from adult rat brains was left untreated (−) or treated with 10 μM nocodazole (Noc) for 40 min at RT (+) prior to velocity sedimentation on a 10–50% discontinuous sucrose gradient as described above. Nitrocellulose membranes were immunoblotted with anti-$GABA_BR1$ or anti-tubulin. (E) An adult rat brain was homogenized to produce a 1000×*g* supernatant (S1). S1 was centrifuged at 16,000×*g* to produce a soluble fraction (S2, lane 1) and a crude membrane fraction (P2, lane 2). S2 was centrifuged at 100,000×*g* to produce a soluble protein fraction (S3, lane 3) and a microsomal pellet (P3, lane 4). Samples were separated by SDS–PAGE and immunoblotted with anti-Marlin-1, anti-$GABA_BR1$, anti-Na^+/K^+ ATPase and anti-kinesin-I antibodies.

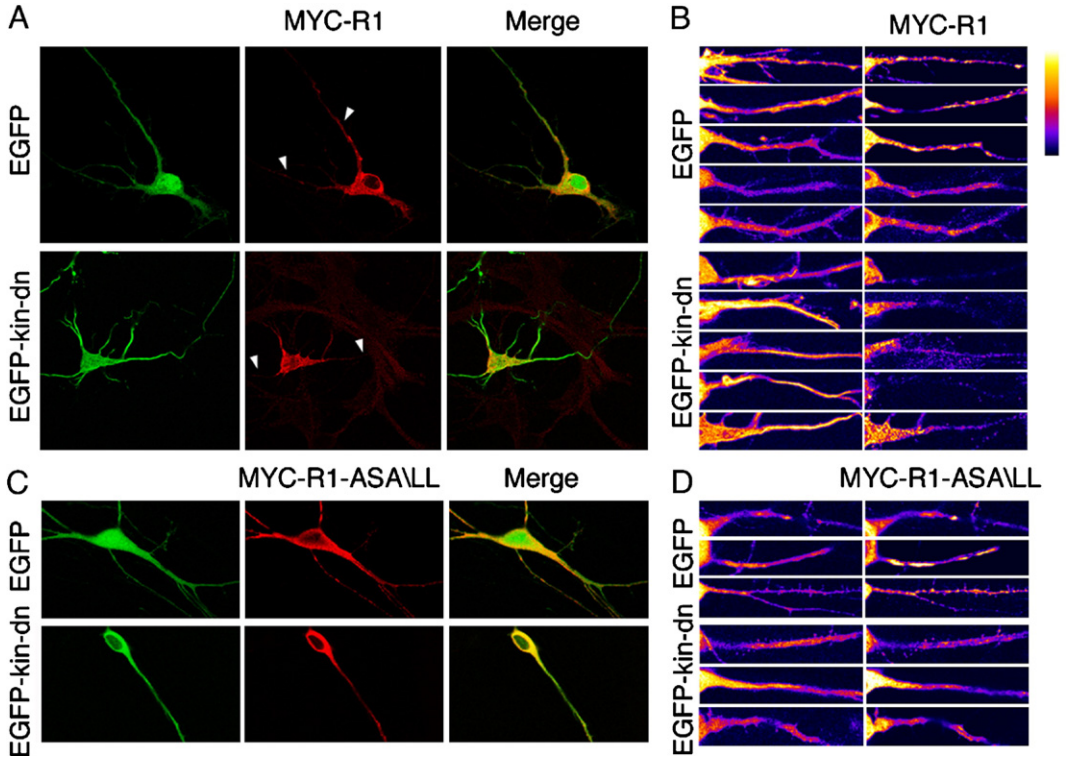

Fig. 6. $GABA_B$ receptor transport is impaired in the presence of EGFP-kin-dn. (A) Cultured hippocampal neurons were co-transfected with MYC-$GABA_B$R1 (MYC-R1) and control EGFP (top panels) or MYC-$GABA_B$R1 and EGFP-kin-dn (lower panels), permeabilized and stained with anti-MYC antibodies. EGFP fluorescence was detected without staining. Anti-mouse Texas Red conjugated secondary antibodies were used to visualize MYC-$GABA_B$R1 (middle). The merge panel is shown (right). Images were obtained using a Zeiss confocal microscope and processed by deconvolution. (B) Representative dendrites taken from the experiment described in panel A. Images show five transfected neurons in a scale of pseudocolor intensity. Top: EGFP (left) and MYC-$GABA_B$R1 (right). Bottom: EGFP-kin-dn (left) and MYC-$GABA_B$R1 (right). (C and D) Same as in panels A and B for hippocampal neurons co-transfected with MYC-$GABA_B$R1-ASA/LL (MYC-R1-ASA/LL) and control EGFP (top panels) or EGFP-kin-dn (lower panels).

and overexpressed protein should displace endogenous cargo from microtubule tracks and thus act as a dominant negative (EGFP-kin-dn). cDNAs were transfected into 15–18 div hippocampal neurons and the distribution of $GABA_B$R1 was examined 24 h later. Neurons transfected with $GABA_B$R1 and control EGFP displayed abundant levels of $GABA_B$R1 in the soma and the subunit reached far into distal dendrites (Fig. 6A, upper panels, arrowheads). On the contrary, a remarkable decrease in the staining of $GABA_B$R1 was observed in dendrites of neurons transfected with EGFP-kin-dn (Fig. 6A, lower panels, arrowheads). The decrease of $GABA_B$R1 in dendrites is evident when multiple projections are compared for relative staining (Fig. 6B). The abundance of EGFP and EGFP-kin-dn throughout the neuronal arbor clearly reflects the integrity of dendrites in these experiments. These results indicate that kinesin-I is necessary for $GABA_B$ receptors transport along dendrites. Interestingly, $GABA_B$R1-ASA/LL, a mutant subunit which escapes the intracellular retention was not affected by EGFP-kin-dn (Figs. 6C and D). Apart from being a control for the use of EGFP-kin-dn, this experiment reveals that the kinesin-I-mediated transport of the $GABA_B$R1 occurs while the subunit is an ER resident.

Discussion

Our results show that Marlin-1 and kinesin-I link $GABA_B$ receptors to the cytoskeleton and regulate receptor transport. This conclusion is explained satisfactorily by the interaction between endogenous Marlin-1, microtubules and kinesin-I and by the tubulin-dependent intracellular movement of Marlin-1. It is also supported by the existence of an intracellular pool of $GABA_B$Rs, presumably in the ER or en route to the plasma membrane, which is sensitive to microtubule integrity and divalent cations. This phenomenon correlates with the displacement of cytoskeletal elements such as tubulin and Marlin-1 from these intracellular compartments. Finally, it is demonstrated by the interaction and regulation of $GABA_B$ receptor transport by kinesin-I.

Marlin-1 and the cytoskeleton

With the use of microtubule stabilizing and destabilizing agents and a protocol of successive cycles of polymerization and depolymerization we have shown that Marlin-1 is a microtubule associated protein in the brain. Canonical microtubule binding motifs are present in MAP and tau proteins, but we have been unable to find such motifs in Marlin-1 (Dehmelt and Halpain, 2005). However, other proteins such as kinesins and myosins associate to microtubules in the absence of conserved motifs (Hirokawa and Takemura, 2005; Cao et al., 2004; Woehlke et al., 1997). Whether similarities exist between the microtubule binding domains of these proteins and Marlin-1 remains to be determined.

Our findings suggest that the interaction with microtubules may not occur directly, but rather through an intermediate protein such as kinesin-I. A previous study has shown that Marlin-1, in addition to its role in binding $GABA_B$Rs, associates with proteins of the Janus kinase family and with polymerized microtubules in Jurkat

and human fibrosarcoma HT-1080 cell lines (Steindler et al., 2004). This report suggests that the amino terminus of Marlin-1, composed primarily of Ccs, is sufficient to mediate its association to microtubules in cell lines. The fact that motor proteins of the kinesin superfamily contain Ccs that mediate self-association and possibly interaction with adaptor proteins, and that the N-terminal of Marlin-1 is sufficient for kinesin-I binding support the hypothesis that kinesin-I may be an intermediate component between Marlin-1 and microtubules.

The intracellular mobility of Marlin-1

The FRAP data in our current study demonstrate that Marlin-1 is a mobile protein in hippocampal neurons. Furthermore, our evidence indicates that there are at least two populations of Marlin-1 in neurons. One population is highly mobile and recovers rapidly after photobleaching, while a second pool fails to recover and corresponds to an immobile protein fraction. Our findings also indicate that approximately equal amounts of mobile and immobile populations of Marlin-1 exist in proximal dendrites. This is consistent with our microscopy data showing the segregation of Marlin-1 and tubulin in the soma of hippocampal neurons. In addition, it is in agreement with our previous data showing that two distinct pools of Marlin-1 can be resolved by sub-cellular fractionation (Couve et al., 2004a). In this context, the immobile pool may correspond to Marlin-1 associated to crude membranes, whereas the mobile pool may correspond to the lighter, intracellular membrane population. In the presence of nocodazole, the population of mobile Marlin-1 disappears completely, indicating unequivocally that mobility of Marlin-1 is controlled by microtubules. Taken together our findings imply that Marlin-1 requires the specific positioning at distant sites of the neuronal arbor and that a dynamic shift between two populations may be an essential aspect of protein function. These results are consistent with the role of Marlin-1 and kinesin-1 in receptor transport.

Since our FRAP studies were carried out in transfected neurons it could be argued that the expression levels affect the outcome of the results. Although neurons with similar fluorescence were chosen for the analysis we have accumulated evidence which strongly argues against this interpretation. First, we have performed FRAP studies in cells transfected with soluble EGFP or membrane-associated myristoylated-EGFP. The extent and kinetics of recovery are much higher for EGFP than myristoylated-EGFP (data not shown). These results indicate that differential recovery depends above all on diffusion barriers. Second, the data for Marlin-1–EGFP in the absence and presence of nocodazole in Fig. 3 show remarkable small dispersion. Considering that fluorescence still varied between cells and that nocodazole had no significant influence on fluorescence, this evidence indicates that the initial fluorescence intensities cannot account for the dramatic differences between control and treated neurons. Third, it is difficult to envision a saturation of the binding sites in abundant cytoskeletal proteins in mature neurons under our overexpression conditions. Indeed, other studies have provided similar arguments to demonstrate that overexpression does not affect FRAP analysis considerably (Zito et al., 2004).

Implications of microtubule polarity in Marlin-1 mobility

The microtubule based mobility of Marlin-1 is mechanistically explained here by the association to kinesin-I. Kinesin-I is a microtubule-dependent plus end motor that mediates the transport of cargo proteins, RNA and organelles in axons and dendrites (Hirokawa and Takemura, 2005).

Several aspects concerning the functional implications of the Marlin-1 and kinesin-I association need to be investigated. First, to conclusively demonstrate that Marlin-1 mobility is dependent on kinesin-I it will be necessary to perform the FRAP analysis in the presence of kinesin-I dominant negative mutants. Second, to understand the implications of Marlin-1 mobility in neuronal polarity the question of directionality of transport will need to be studied in detail. In this report, we have demonstrated that Marlin-1 moves bidirectionally. Since microtubules are polarized in the axon and distal dendrites but show no preferred orientation in proximal dendrites it remains to be established how the different neuronal domains alter the mobility of Marlin-1. The specificity of the Marlin-1/kinesin-I interaction allows us to predict a unidirectional movement in the axon and in distal dendrites. Undoubtedly the mechanisms responsible for directional $GABA_B$ receptor transport will need to be studied taking this information into account.

Other functions of Marlin-1

A recent study has suggested that recombinant Marlin-1 affects the stability of microtubules in tissue culture cells (Steindler et al., 2004). It will be challenging to reconcile the roles of Marlin-1 in microtubule stability and microtubule-dependent movement. However, it has been reported that some members of the kinesin superfamily, namely M-kinesins, function in protein transport and are also able to depolymerize microtubules (Hirokawa and Takemura, 2005). Whether this dual function applies to a Marlin-1/kinesin-I complex remains to be established.

In a previous study we demonstrated that Marlin-1 functioned as an RNA adaptor protein (Couve et al., 2004a). The close association between RNA binding proteins, the synthetic machinery and the cytoskeleton has become an area of intense research. For example, TB-RBP (testis/brain RNA binding protein), Spnr (spermatid perinuclear RNA binding protein), Staufen and Vg1 all bind RNA and the tubulin cytoskeleton (Jansen, 1999). Some of these may participate in linking specific mRNAs or poly(A) RNA to microtubules, while others may have a more direct role in translation. The relationship between the RNA and microtubule binding properties of Marlin-1 remains a challenging problem to tackle.

Neurotransmitter receptors, molecular motors and adaptor proteins

The role of the cytoskeleton, molecular motors and adaptor proteins in neurotransmitter receptor transport has been widely explored. For glutamate receptors, the protein GRIP1 has been shown to function as an adaptor between the AMPA receptor subunit GluR2 and members of the KIF5 (kinesin-I) subfamily (Setou et al., 2002), while for the NR2B subunit of the NMDA a molecular complex formed by Lin7, Lin2 and Lin10 has been shown function as an adaptor with the molecular motor KIF17 and direct the complex to post-synaptic sites (Guillaud et al., 2003). The existence of multiple adaptor proteins operating on fewer molecular motors has also received attention (Hirokawa and Takemura, 2005). In this respect, the difference between ionotropic and $GABA_B$ receptors is evident. Recently, GRIF-1, a $GABA_A$ interacting protein has been described to mediate the association with kinesin-I subtypes (Brickley et al., 2005). Likewise, gephyrin

has been shown to interact with Dlc1 and Dlc2, two proteins of the dynein motor complex (Fuhrmann et al., 2002). In this study we provide evidence that kinesin-I also mediates the transport of $GABA_B$ receptors. Therefore, the proteins that act as adaptors seem specific for each receptor type.

The participation of other intermediate proteins that link receptors to the cytoskeleton has been explored for the ionotropic GABA receptors, namely $GABA_A$ and $GABA_C$ receptors. In this respect, at least four proteins have been identified, these correspond to gephyrin, GABARAP, PLICs and MAP1B (Moss and Smart, 2001). During the formation or modification of inhibitory synapses gephyrin promotes the clustering of $GABA_A$ receptors while GABARAP and PLICs link receptors to the cytoskeleton during still poorly defined intracellular trafficking events. Likewise, MAP1B has been suggested to anchor $GABA_C$ receptors to the cytoskeleton in bipolar cells of the retina. Whatever the consequences of these interactions may be it is clear that the set of proteins that control $GABA_BR$ association to the cytoskeleton are different from those employed by ionotropic GABA receptors. This difference is not difficult to explain as $GABA_BRs$, contrary to $GABA_A$ or $GABA_C$ receptors, are abundant in presynaptic terminals and extrasynaptic sites on excitatory and inhibitory synapses (Kulik et al., 2002; Kulik et al., 2003).

Transport of $GABA_BRs$

The $GABA_BR1$ subunit is essential for $GABA_BR$ function and has been implicated in dendritic and axonal targeting of $GABA_BRs$ (Vigot et al., 2006). Interestingly it contains an ER retention motif and it is retained in the ER when overexpressed in neurons (Couve et al., 1998; Filippov et al., 2000). Here we demonstrate that kinesin-I is required for $GABA_BR1$ entry into dendrites. Importantly, kinesin-I does not affect the distribution of $GABA_BR1$-ASA/LL, a mutant receptor that bypasses at least two checkpoints in the secretory pathway (Restituito et al., 2005). Thus, an interesting possibility that arises from our results is that receptors may be transported along dendrites while residing in the reticular or vesicular ER. Interestingly, the movement of ER resident proteins is microtubule- and kinesin-dependent (Bannai et al., 2004). Moreover, the velocities of the ER movement are similar to the ones described here. These observations suggest that $GABA_BR$ subunits may be synthesized and transported independently into the dendritic arbor and subsequently assembled and inserted into synaptic or extrasynaptic sites. How different splice variants acquire axonal or dendritic localization remains to be determined.

Polarized transport and molecular motors

Although kinesins mediate axonal and dendritic transport, they have been shown to have specific effects on dendritic steering of cargo (Miki et al., 2001). Clearly, the interaction with microtubules and dendritic steering are not sufficient to account for efficient delivery of neurotransmitter receptors to postsynaptic sites. This conclusion is supported by the co-localization studies between KIF17 and synaptic markers, which demonstrate that KIF17 does not reach the proximity of the PSD (Guillaud et al., 2003). Interestingly, the final stages seem to be modulated preferentially by the actin cytoskeleton. In agreement with these findings our data clearly show that Marlin-1 does not enter the actin rich cortex in neurons, and thus that functions prior to synaptic (or extrasynaptic) delivery. Whether the cargo is transferred to an actin based motor system and how this occurs remains a topic of investigation not just for $GABA_B$ but for many neurotransmitter receptors.

Concluding remarks

In this report we have not performed single-particle tracking to determine precisely the velocity of Marlin-1–EGFP movement within dendrites nor have we investigated the kinetics of $GABA_B$ receptor movement. However, under control conditions 50% recovery of Marlin-1–EGFP occurred in ~150 s, similar to the rates of FRAP recovery of the AMPA receptor subunits GluR1–EGFP and GluR2–EGFP in transfected hippocampal neurons (Perestenko and Henley, 2003). Although the experiments were performed at different temperatures in ours and the reported study (22 °C and 37 °C, respectively), previous data indicates that conventional kinesin only doubles its velocity in this temperature range, making both data sets comparable (Bohm et al., 2000). These results suggest that cargo proteins such as AMPA receptors, Marlin-1 and presumably $GABA_BRs$ may be transported along neurites with similar kinetics.

Experimental methods

Reagents

Paclitaxel (Taxol™) and nocodazole were purchased from Sigma (St. Louis, MO).

Plasmids

The constructs containing MYC–$GABA_BR1$, FLAG–Marlin-1 and domains of Marlin-1 tagged with FLAG or MYC epitopes in the pRK5 mammalian expression vector have been described previously (Couve et al., 2004a). The kinesin dominant negative construct (EGFP-kin-dn) was kindly provided by S. Kindler. EGFP-kin-dn corresponds to nucleotides 1–990 of rat KIF5C subcloned into pEGFP-N3 using *Hind*III and *Bam*HI (Clontech Laboratories, Palo Alto, CA).To produce Marlin-1–EGFP, Marlin-1 was amplified using specific 5′ (GCAGATCTATGTCGAA-GAAAGGCCGGAG) and 3′ (GCAAGCTTGCTTTACATGAATTTCAG) primers. The PCR product was incorporated into pGEM-T-Easy (Promega, Madison, WI) and subcloned into pEGFP-C1 (Clontech, Mountain View, CA) using *Bgl*II and *Hind*III restriction sites. All DNA manipulations and fidelity of DNA constructs were verified by DNA sequencing.

Antibodies

Marlin-1 antibodies have been described previously (Couve et al., 2004a). Chicken $GABA_BR1$ antibodies were kindly provided by S. Moss (Kuramoto et al., 2007). Kinesin-II antibodies were kindly provided by S. Kindler. Monoclonal dynein (intermediate chain), β-tubulin, anti-FLAG and anti-MYC antibodies were purchased from Sigma (St. Louis, MO). Guinea-pig $GABA_B$ receptor and kinesin-I heavy chain antibodies were purchased from Chemicon (Temecula, CA). Monoclonal 3E6 GFP antibodies were purchased from Molecular Probes, Invitrogen (Eugene, OR). The secondary anti-mouse and anti-rabbit antibodies conjugated to Texas Red (TR), fluorescein isothiocyanate (FITC) and horseradish peroxidase (HRP) were purchased from Jackson Immuno Research Laboratories (West Grove, PA).

Animals

Adult pregnant female Sprague-Dawley rats and adult BALB/c mice were purchased from the Central Animal Facility at Universidad Católica de Chile and killed by asphyxia in a CO_2 chamber according to the Guide for

Care and Use of Laboratory Animals (copyright 1996, National Academy of Science).

Neuronal cultures and transfection

Primary cultures of rat hippocampal neurons were obtained from E18 rats and maintained as described previously (Goslin and Banker, 1991). Neurons were transfected after 8–10 div using the Lipofectamine Reagent (Invitrogen) following instructions from the supplier. Alternatively neurons were transfected after 15–18 div using the calcium phosphate method (Xia et al., 1996). Neurons were imaged 24–48 h after transfection.

Brain fractionation and velocity sedimentation on sucrose gradients

Adult rat brains were homogenized in 10 volumes of 5 mM Tris–Cl pH 7.4 containing 0.32 M sucrose using 50 strokes in a glass-Teflon homogenizer. The homogenate was centrifuged at 1400×*g* for 10 min and the supernatant was saved (S1.1). The pellet was homogenized again in the same buffer and centrifuged at 1400×*g* for 10 min at 4 °C (S1.2). The resulting supernatants were pooled (S1) and centrifuged at 16,000×*g* for 30 min at 4 °C to obtain a crude membrane preparation (P2) and a post-mitochondrial fraction (S2). The membrane fraction (P2) was washed three times in 50 mM Tris–Cl pH 7.4, 0.1% phenylmethylsulfonyl fluoride, 10 μg/ml leupeptin, 10 μg/ml pepstatin, 10 μg/ml antipain and resuspended at a concentration of 5 mg/ml. S2 was spun at 100,000×*g* for 30 min at 4 °C. The resulting supernatant (S3) was saved and the pellet (P3) was resuspended in an equivalent volume of 50 mM Tris–Cl pH 7.4. The resuspended P3 fraction was loaded on top of a 10–50% discontinuous sucrose density gradient and centrifuged at 40,000×*g* for 2 h. Fractions were collected and samples were denatured, separated by SDS–PAGE and transferred to nitrocellulose membranes. For treatments the P3 fraction was treated with 30 mM EDTA for 30 min at 4 °C, 1 U/μl RNAse T1 plus 0.044 U/μl RNAse A for 10 min at RT or 1% DOC for 30 min at RT.

Microtubule association assays

Adult rat brains were homogenized and fractionated as described above. The resuspended P3 fraction was divided in three. Aliquots were left untreated or treated with 20 μM Taxol (plus 1 mM GTP) or 10 μM nocodazole for 40 min at RT. Aliquots were then centrifuged at 100,000×*g* for 30 min at 4 °C. The supernatants were saved and the resulting pellets containing polymerized microtubules were resuspended in an equal volume of 50 mM Tris–Cl pH 7.4 buffer. Samples were denatured, separated by SDS–PAGE and transferred to nitrocellulose membranes.

Immunoblot, immunoprecipitation, immunofluorescence and image analyses

Immunoprecipitations were carried out as described previously from S1 or S16 brain fractions (Couve et al., 2001). Immunofluorescence and immunoblots were performed as described previously (Couve et al., 2002). Immunoblot reactions were visualized using enhanced chemiluminescence (ECL, Amersham Pharmacia Biotech, Buckinghamshire, UK). For immunofluorescence coverslips were examined using a Zeiss, Pascal 5 axiovert 200 confocal microscope and LSM 5 3.2 image capture and analysis software. Image processing was performed using the Huygens deconvolution software and IDL co-localization and 3D reconstruction software.

Fluorescence recovery after photobleaching (FRAP)

All experiments were performed at ambient temperature in a 22 °C equilibrated microscopy suite. 24 h after transfection, glass coverslips containing neurons were transferred to an imaging chamber in Tyrode's solution (124 mM NaCl, 5 mM KCl, 2 mM $CaCl_2$, 1 mM $MgCl_2$, 30 mM glucose, 25 mM HEPES pH 7.4). EGFP or Marlin-1–EGFP positive cells were scanned with an Argon 488 nm laser at 5–10% power to determine a measurement of initial fluorescence intensity. Regions of interest (ROIs) of ~9 μm^2 were selected and placed over a principal dendrite of a green fluorescent cell. ROIs were then subjected to 10 cycles with the Argon 488 nm laser at 100% power to photo-bleach the ROI. The fluorescence recovery of the ROI was subsequently measured every 5–30 s at 2–5% laser power by imaging the entire cell. The procedure was repeated independently in ~10 cells/coverslip. Samples were examined using a Zeiss, Pascal 5 axiovert 200 confocal microscope and LSM 5 3.2 image capture and analysis software. Data sets were obtained from multiple images using the Image J software. A box of ~3 μm^2 was selected within the original photo-bleached ROI and placed at a distance of 1 μm from the edge of the non-bleached region. The mean intensity of the photobleached area was obtained for every time frame and the value was normalized to the intensity of the same area in the control frame before photobleaching. An average curve was obtained and plotted against time. For nocodazole treatments, hippocampal neurons were incubated with 100 μM nocodazole for 3 h before imaging. Only cells with normal morphology were chosen for our analysis and we ignored the saturated levels of fluorescence in the neuronal soma to provide the best conditions to monitor EGFP and Marlin-1–EGFP in projections.

Acknowledgments

We would like to thank Elvis Acevedo for technical assistance. R.L.V. funded by Ph.D. fellowship from CONICYT. O.A.R. funded by Ph.D. fellowship from MECESUP. S.H funded by FONDECYT 1060890. A.C. funded by FONDECYT 1040083, Iniciativa Científica Milenio ICM-P04-068-F and FONDAP 15010006.

Appendix A. Supplementary data

Supplementary data associated with this article can be found, in the online version, at doi:10.1016/j.mcn.2007.04.008.

References

Bailey, C.H., Kandel, E.R., Si, K., 2004. The persistence of long-term memory. A molecular approach to self-sustaining changes in learning-induced synaptic growth. Neuron 30, 49–57.

Bannai, H., Inoue, T., Nakayama, T., Hattori, M., Mikoshiba, K., 2004. Kinesin dependent, rapid, bi-directional transport of ER sub-compartment in dendrites of hippocampal neurons. J. Cell Sci. 117 (Pt 2), 163–175.

Bettler, B., Kaupmann, K., Mosbacher, J., Gassmann, M., 2004. Molecular structure and physiological functions of GABA(B) receptors. Physiol. Rev. 84, 835–867.

Brickley, K., Smith, M.J., Beck, M., Stephenson, F.A., 2005. GRIF-1 and OIP106, members of a novel gene family of coiled-coil domain proteins, association in vivo and in vitro with kinesin. J. Biol. Chem. 280, 14723–14732.

Brock, C., Boudier, L., Maurel, D., Blahos, J., Pin, J.P., 2005. Assembly-dependent surface targeting of the heterodimeric $GABA_B$ receptor is controlled by COPI but not 14-3-3. Mol. Biol. Cell 16, 5572–5578.

Bohm, K.J., Stracke, R., Baum, M., Zieren, M., Unger, E., 2000. Effect of temperature on kinesin-driven microtubule gliding and kinesin ATPase activity. FEBS Lett. 466, 59–62.

Burkhard, P., Stetefeld, J., Strelkov, S.V., 2001. Coiled coils, a highly versatile protein folding motif. Trends Cell Biol. 11, 82–88.

Cao, T.T., Chang, W., Masters, S.E., Mooseker, M.S., 2004. Myosin-Va binds to and mechanochemically couples microtubules to actin filaments. Mol. Biol. Cell 15, 151–161.

Clem, R.L., Barth, A., 2006. Pathway-specific trafficking of native AMPARs by in vivo experience. Neuron 49, 663–670.

Collingridge, G.L., Isaac, J.T., Wang, Y.T., 2004. Receptor trafficking and synaptic plasticity. Nat. Rev., Neurosci. 5, 952–962.

Correa, S.A., Munton, R., Nishimune, A., Fitzjohn, S., Henley, J.M., 2004. Development of $GABA_B$ subunits and functional $GABA_B$ receptors in rat cultured hippocampal neurons. Neuropharmacology 47, 475–484.

Couve, A., Filippov, A.K., Connolly, C.N., Bettler, B., Brown, D.A., Moss, S.J., 1998. Intracellular retention of recombinant $GABA_B$ receptors. J. Biol. Chem. 273, 26361–26367.

Couve, A., Kittler, J.T., Uren, J.M., Calver, A.R., Pangalos, M.N., Walsh, F.S., Moss, S.J., 2001. Association of GABA(B). Receptors and members of the 14-3-3 family of signaling proteins. Mol. Cell. Neurosci. 17, 317–328.

Couve, A., Thomas, P., Calver, A.R., Hirst, W.D., Pangalos, M.N., Walsh, F.S., Smart, T.G., Moss, S.J., 2002. Cyclic AMP-dependent protein kinase phosphorylation facilitates GABA(B). Receptor–effector coupling. Nat. Neurosci. 5, 415–424.

Couve, A., Restituito, S., Brandon, J.M., Charles, K.J., Bawagan, H., Freeman, K.B., Pangalos, M.N., Calver, A.R., Moss, S.J., 2004a. Marlin-1, a novel RNA-binding protein associates with GABA receptors. J. Biol. Chem. 279, 13934–13943.

Couve, A., Calver, A.R., Fairfax, B., Moss, S.J., Pangalos, M.N., 2004b. Unravelling the unusual signalling properties of the GABA(B) receptor. Biochem. Pharmacol. 68, 1527–1536.

Craig, A.M., Boudin, H., 2001. Molecular heterogeneity of central synapses, afferent and target regulation. Nat. Neurosci. 4, 569–578.

Dehmelt, L., Halpain, S., 2005. The MAP2/Tau family of microtubule-associated proteins. Genome Biol. 6, 204.

Filippov, A.K., Couve, A., Pangalos, M.N., Walsh, F.S., Brown, D.A., Moss, S.J., 2000. Heteromeric assembly of GABA(B)R1 and GABA(B)R2 receptor subunits inhibits Ca(2+) current in sympathetic neurons. J. Neurosci. 20, 2867–2874.

Fuhrmann, J.C., Kins, S., Rostaing, P., El Far, O., Kirsch, J., Sheng, M., Triller, A., Betz, H., Kneussel, M., 2002. Gephyrin interacts with Dynein light chains 1 and 2, components of motor protein complexes. J. Neurosci. 22, 5393–5402.

Goslin, K., Banker, G., 1991. Rat hippocampal neurons in low-density cultures. In: Banker, G., Goslin, K. (Eds.), Culturing Nerve Cells. MIT, Cambridge, MA, pp. 251–281.

Guillaud, L., Setou, M., Hirokawa, N., 2003. KIF17 dynamics and regulation of NR2B trafficking in hippocampal neurons. J. Neurosci. 23, 131–140.

Hirokawa, N., Takemura, R., 2005. Molecular motors and mechanisms of directional transport in neurons. Nat. Rev., Neurosci. 6, 201–214.

Jansen, R.P., 1999. RNA–cytoskeletal associations. FASEB J. 13, 455–466.

Kittler, J.T., McAinsh, K., Moss, S.J., 2002. Mechanisms of $GABA_A$ receptor assembly and trafficking, implications for the modulation of inhibitory neurotransmission. Mol. Neurobiol. 26, 251–268.

Kulik, A., Nakadate, K., Nyiri, G., Notomi, T., Malitschek, B., Bettler, B., Shigemoto, R., 2002. Distinct localization of GABA(B) receptors relative to synaptic sites in the rat cerebellum and ventrobasal thalamus. Eur. J. Neurosci. 15, 291–307.

Kulik, A., Vida, I., Lujan, R., Haas, C.A., Lopez-Bendito, G., Shigemoto, R., Frotscher, M., 2003. Subcellular localization of metabotropic GABA (B) receptor subunits GABA(B1a/b) and GABA(B2) in the rat hippocampus. J. Neurosci. 23, 11026–11035.

Kuramoto, N., Wilkins, M.E., Fairfax, B.P., Revilla-Sanchez, R., Terunuma, M., Tamaki, K., Iemata, M., Warren, N., Couve, A., Calver, A., Horvath, Z., Freeman, K., Carling, D., Huang, L., Gonzales, C., Cooper, E., Smart, T.G., Pangalos, M.N., Moss, S.J., 2007. Phospho-dependent functional modulation of GABA(B) receptors by the metabolic sensor AMP-dependent protein kinase. Neuron 53, 233–247.

Lee, S.H., Valtschanoff, J.G., Kharazia, V.N., Weinberg, R., Sheng, M., 2001. Biochemical and morphological characterization of an intracellular membrane compartment containing AMPA receptors. Neuropharmacology 41, 680–692.

Miki, H., Setou, M., Kaneshiro, K., Hirokawa, N., 2001. All kinesin superfamily protein, KIF, genes in mouse and human. Proc. Natl. Acad. Sci. U. S. A. 98, 7004–7011.

Moss, S.J., Smart, T.G., 2001. Constructing inhibitory synapses. Nat. Rev., Neurosci. 2, 240–250.

Mott, D.D., Lewis, D.V., 1994. The pharmacology and function of central $GABA_B$ receptors. Int. Rev. Neurobiol. 36, 97–223.

Perestenko, P.V., Henley, J.M., 2003. Characterization of the intracellular transport of GluR1 and GluR2 alpha-amino-3-hydroxy-5-methyl-4-isoxazole propionic acid receptor subunits in hippocampal neurons. J. Biol. Chem. 278, 43525–43532.

Pfister, K.K., Wagner, M.C., Stenoien, D.L., Brady, S.T., Bloom, G.S., 1989. Monoclonal antibodies to kinesin heavy and light chains stain vesicle-like structures, but not microtubules, in cultured cells. J. Cell Biol. 108, 1453–1463.

Pin, J.P., Kniazeff, J., Binet, V., Liu, J., Maurel, D., Galvez, T., Duthey, B., Havlickova, M., Blahos, J., Prezeau, L., Rondard, P., 2004. Activation mechanism of the heterodimeric GABA(B) receptor. Biochem. Pharmacol. 68, 1565–1572.

Pontier, S.M., Lahaie, N., Ginham, R., St-Gelais, F., Bonin, H., Bell, D.J., Flynn, H., Trudeau, L.E., McIlhinney, J., White, J.H., Bouvier, M., 2006. Coordinated action of NSF and PKC regulates $GABA_B$ receptor signaling efficacy. EMBO J. 25, 2698–2709.

Restituito, S., Couve, A., Bawagan, H., Jourdain, S., Pangalos, M.N., Calver, A.R., Freeman, K.B., Moss, S.J., 2005. Multiple motifs regulate the trafficking of GABA(B) receptors at distinct checkpoints within the secretory pathway. Mol. Cell. Neurosci. 28, 747–756.

Setou, M., Seog, D.H., Tanaka, Y., Kanai, Y., Takei, Y., Kawagishi, M., Hirokawa, N., 2002. Glutamate-receptor-interacting protein GRIP1 directly steers kinesin to dendrites. Nature 417, 83–87.

Soto, C., Rodriguez, P.H., Monasterio, O., 1996. Calcium and gadolinium ions stimulate the GTPase activity of purified chicken brain tubulin through a conformational change. Biochemistry 35, 6337–6344.

Steindler, C., Li, Z., Algarte, M., Alcover, A., Libri, V., Ragimbeau, J., Pellegrini, S., 2004. Jamip1, marlin-1 defines a family of proteins interacting with janus kinases and microtubules. J. Biol. Chem. 279, 43168–43177.

Tan, C.M., Brady, A.E., Nickols, H.H., Wang, Q., Limbird, L.E., 2004. Membrane trafficking of G protein-coupled receptors. Annu. Rev. Pharmacol. Toxicol. 44, 559–609.

Vigot, R., Barbieri, S., Brauner-Osborne, H., Turecek, R., Shigemoto, R., Zhang, Y.P., Lujan, R., Jacobson, L.H., Biermann, B., Fritschy, J.M., Vacher, C.M., Muller, M., Sansig, G., Guetg, N., Cryan, J.F., Kaupmann, K., Gassmann, M., Oertner, T.G., Bettler, B., 2006. Differential compartmentalization and distinct functions of $GABA_B$ receptor variants. Neuron 50, 589–601.

Woehlke, G., Ruby, A.K., Hart, C.L., Ly, B., Hom-Booher, N., Vale, R.D., 1997. Microtubule interaction site of the kinesin motor. Cell 90, 207–216.

Xia, Z., Dudek, H., Miranti, C.K., Greenberg, M.E., 1996. Calcium influx via the NMDA receptor induces immediate early gene transcription by a MAP kinase/ERK-dependent mechanism. J. Neurosci. 16, 5425–5436.

Zito, K., Knott, G., Shepherd, G.M., Shenolikar, S., Svoboda, K., 2004. Induction of spine growth and synapse formation by regulation of the spine actin cytoskeleton. Neuron 44, 321–334.